

STRONG CLUSTERING OF HIGH-REDSHIFT $\text{Ly}\alpha$ FOREST ABSORPTION SYSTEMSA. FERNÁNDEZ-SOTO,^{1,2} K. M. LANZETTA,³ X. BARCONS,¹ R. F. CARSWELL,⁴ J. K. WEBB,⁵ AND A. YAHIL³*Received 1995 November 15; accepted 1996 January 23*

ABSTRACT

We use new observations of very weak C IV absorption lines associated with high-redshift $\text{Ly}\alpha$ absorption systems to measure the high-redshift $\text{Ly}\alpha$ line two-point correlation function (TPCF). These very weak C IV absorption lines trace small-scale velocity structure that cannot be resolved by $\text{Ly}\alpha$ absorption lines. We find that (1) high-redshift $\text{Ly}\alpha$ absorption systems with $N(\text{H I}) > 3 \times 10^{14} \text{ cm}^{-2}$ are strongly clustered in redshift, (2) previous measurements of the $\text{Ly}\alpha$ line TPCF underestimated the actual clustering of the absorbers due to unresolved blending of overlapping velocity components, (3) the present observations are consistent with the hypothesis that clustering of $\text{Ly}\alpha$ absorption systems extends to lower column densities, but maybe with smaller amplitude in the correlation function, and (4) the observed clustering is broadly compatible with that expected for galaxies at $z \sim 2\text{--}3$. We interpret these results as suggesting that many or most $\text{Ly}\alpha$ absorbers may arise in galaxies even at high redshifts, and, therefore, that the $\text{Ly}\alpha$ forest probes processes of galaxy formation and evolution for redshifts $z \lesssim 5$.

Subject headings: galaxies: evolution — quasars: absorption lines

1. INTRODUCTION

The observational result that high-redshift $\text{Ly}\alpha$ absorption systems appear not to cluster strongly in redshift (see, e.g., Sargent et al. 1980) has driven most discussion about the origin of the $\text{Ly}\alpha$ forest. This result has generally been interpreted as evidence that high-redshift $\text{Ly}\alpha$ absorbers arise in intergalactic clouds rather than in galaxies. Recent studies of the relationship between $\text{Ly}\alpha$ absorbers and galaxies at redshifts $z \lesssim 1$, however, directly demonstrate that many or most low-redshift $\text{Ly}\alpha$ absorbers [or at least those satisfying $W_{\text{rest}}(\text{Ly}\alpha) \gtrsim 0.3 \text{ \AA}$] arise in galaxies rather than in intergalactic clouds (Lanzetta et al. 1995). Why is it that $\text{Ly}\alpha$ absorbers appear not to cluster strongly in redshift whereas low-redshift $\text{Ly}\alpha$ absorbers appear to arise in galaxies?

One suggestion is that there exist two distinct populations of $\text{Ly}\alpha$ absorbers: a rapidly evolving, unclustered, intergalactic population that dominates at high redshifts, and a slowly evolving, clustered, galactic population that dominates at low redshifts (see, e.g., Bahcall et al. 1996). Another possibility is that previous measurements of the high-redshift $\text{Ly}\alpha$ two-point correlation function (TPCF) have underestimated the actual clustering of the absorbers—presumably due to unresolved blending of overlapping velocity components—and $\text{Ly}\alpha$ absorbers arise in galaxies at all epochs.

Here we examine the second of these possibilities, that previous measurements of the high-redshift $\text{Ly}\alpha$ TPCF have underestimated the actual clustering of the absorbers, using new observations of very weak C IV absorption lines associated with high-redshift $\text{Ly}\alpha$ absorbers (Cowie et al. 1995, hereafter

CSKH) (§ 2). These very weak C IV absorption lines trace small-scale velocity structures that cannot be resolved by $\text{Ly}\alpha$ absorption lines because (1) the atomic weight of C is 12 times the one of H, so the thermal broadening of C IV absorption lines is 3.5 times smaller than that of $\text{Ly}\alpha$ lines, and (2) C IV absorption lines suffer far less saturation because of the difference in column densities. We show that the C IV lines indeed help to reveal the underlying velocity correlation of the $\text{Ly}\alpha$ systems, and that this same velocity structure is blended away in the $\text{Ly}\alpha$ data (§ 3). We conclude with a comparison of the derived velocity clustering of the $\text{Ly}\alpha$ absorbers with that of galaxies at the present epoch (§ 4).

2. DATA

The observations by CSKH consist of high spectral resolution (FWHM $\approx 8 \text{ km s}^{-1}$), high signal-to-noise ratio (S/N ≈ 50 per resolution element) spectra of three QSOs obtained with the Keck telescope and the HIRES spectrograph. The observations generally cover both the $\text{Ly}\alpha$ and the corresponding C IV wavelength regions and are sensitive to C IV absorption lines arising in C IV column densities as low as $N(\text{C IV}) \approx 10^{12} \text{ cm}^{-2}$.

From the observations, CSKH selected a complete sample of 38 $\text{Ly}\alpha$ absorption lines satisfying $N(\text{H I}) \geq 2 \times 10^{14} \text{ cm}^{-2}$. They then eliminated seven of these absorption lines due to contamination by unrelated metal absorption lines or lack of coverage of the corresponding C IV wavelength region or because the lines produce corresponding Lyman-limit absorption [which indicates $N(\text{H I}) \gtrsim 2 \times 10^{17} \text{ cm}^{-2}$]. The resulting sample thus contains 31 $\text{Ly}\alpha$ absorption lines satisfying $3 \times 10^{14} \text{ cm}^{-2} \leq N(\text{H I}) \leq 2 \times 10^{17} \text{ cm}^{-2}$. For each member of this sample, they searched the corresponding C IV wavelength region for C IV absorption lines and applied a Voigt profile fitting procedure to the identified C IV absorption lines to measure redshifts, Doppler parameters, and column densities.

Here we use the absorption system parameters derived by CSKH in their profile analysis, which are summarized in their Table 1a. The average redshift of the absorbers is $\langle z \rangle = 2.6$, the median column density of the absorbers is $N(\text{H I}) = 8.1 \times 10^{14}$

¹ Instituto de Física de Cantabria, Consejo Superior de Investigaciones Científicas, Universidad de Cantabria, Facultad de Ciencias, 39005 Santander, Spain.

² Departamento de Física Moderna, Universidad de Cantabria, 39005 Santander, Spain.

³ Astronomy Program, Department of Earth and Space Sciences, State University of New York at Stony Brook, Stony Brook, NY 11794-2100.

⁴ Institute of Astronomy, University of Cambridge, Cambridge CB3 0HA, UK.

⁵ School of Physics, University of New South Wales, P.O. Box 1, Kensington, NSW, Australia.

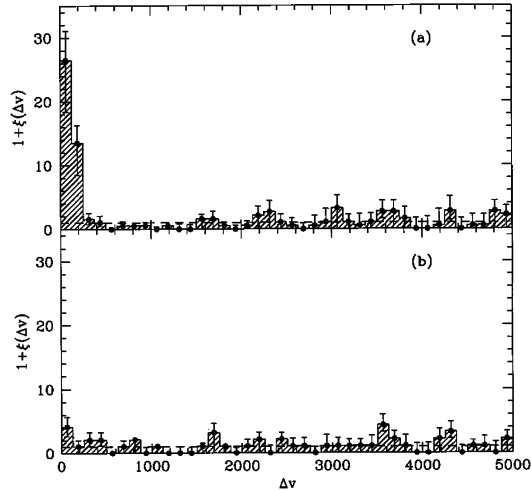


FIG. 1.—High-redshift Ly α TPCF as traced by very weak C IV absorption lines (*upper panel*) and as traced by Ly α absorption lines (*lower panel*).

cm^{-2} , and the typical C IV/H I ratio of the absorbers is 3×10^{-3} . Of the final sample of 31 Ly α absorption lines, 15 are observed to have associated C IV absorption, of which six show small-scale velocity structure with between two and nine velocity components per Ly α absorption line.

3. ANALYSIS

3.1. High-Redshift Ly α Two-point Correlation Function

Our primary assumption is that very weak C IV absorption lines trace small-scale velocity structure that cannot be resolved by Ly α absorption lines. Hence the goal of the analysis is to measure the high-redshift Ly α TPCF by using very weak C IV absorption lines instead of the Ly α absorption lines themselves.

To do this we use the results summarized in Table 1a of CSKH. In cases where CSKH identified one or more C IV absorption lines with a single Ly α absorption line, we use the redshifts of all C IV absorption lines in the analysis. In cases where CSKH identified no C IV absorption lines with a single Ly α absorption line, we use the single redshift of the Ly α absorption line in the analysis. This procedure yields a total of 52 absorption redshifts. We then use these absorption redshifts to construct the Ly α line TPCF by normalizing the distribution of velocity pairs with respect to an unclustered distribution of redshifts.

The results are shown in Figure 1, which plots in the upper panel the high-redshift Ly α line TPCF as traced by C IV absorption lines. (The error bars shown in Fig. 1 are based on a modified “bootstrap” technique that yields approximately correct results even for correlated data. Details of this technique will be presented elsewhere.) It is clear from Figure 1 that the high-redshift Ly α TPCF indicates very strong clustering on velocity scales $\lesssim 250 \text{ km s}^{-1}$. We therefore conclude that high-redshift Ly α absorption systems with $N(\text{H I}) > 3 \times 10^{14} \text{ cm}^{-2}$ are strongly clustered in redshift.

3.2. Blending of Overlapping Velocity Components

The results of § 3.1 demonstrate that high-redshift Ly α absorption systems with $N(\text{H I}) > 3 \times 10^{14} \text{ cm}^{-2}$ are strongly clustered in redshift, whereas all previous analyses have found that they are either unclustered (Sargent et al. 1980) or only

very weakly clustered in redshift (see, e.g., Webb 1987; Barcons & Webb 1991). How are these results compatible?

To examine this issue, we apply the standard method of measuring the Ly α TPCF to models of the Ly α absorption lines observed by CSKH. We first generate a set of Ly α absorption lines according to the results in Table 1a of CSKH. We adopt a constant C IV/H I ratio of 3×10^{-3} and assume that the Doppler parameters are due to thermal motions, convolve the synthetic absorption lines with the appropriate instrumental response, and add noise to match the actual S/N ratio of the observations. Next, we fit the resulting synthetic spectra using the Voigt profile fitting routine described previously by Lanzetta & Bowen (1992). For each absorption line we add velocity components until the decrease in χ^2 is smaller than the accompanying decrease in degrees of freedom, ν . Finally, we construct the Ly α TPCF according to the procedures described in the previous section, but this time using the fitted redshifts instead of the actual redshifts.

The results are shown in Figure 1, which plots in the lower panel the high-redshift Ly α TPCF as traced by Ly α absorption lines. It is clear that the Ly α absorption lines cannot reveal the strong clustering indicated by the C IV absorption lines. The lower panel of Figure 1 may be directly compared with the high-redshift Ly α TPCF presented by Hu et al. (1995); both use observations of nearly the same quality, and both obtain practically identical results. Note that our stopping criterion for velocity components, $\Delta\chi^2 < \Delta\nu$ purposely allows even marginally significant lines to be included. If no correlation is obtained even with this generous criterion, it certainly will not be found with a more conservative one. We therefore conclude that previous measurements of the high-redshift Ly α TPCF have underestimated the actual clustering of the absorbers due to unresolved blending of overlapping velocity components.

3.3. Extension to Lower Column Densities

The results of the previous section demonstrate that previous measurements of the high-redshift Ly α TPCF of absorbers with $N(\text{H I}) > 3 \times 10^{14} \text{ cm}^{-2}$ have underestimated the actual clustering of the absorbers. Can this result extend to lower column densities for which blending is presumably weaker?

To examine this issue, we repeat the analysis described in the previous section for Ly α lines generated in two different ways. For the first simulation we assume that the C IV Doppler parameter b is entirely due to thermal motion, so $b(\text{H I}) = \sqrt{12b(\text{C IV})}$, and we reduce the H I column densities by a factor of 100 with respect to the original ones. An example of just how a Voigt profile fit to high spectral resolution, high S/N observations can underestimate the actual number of velocity components comprising an absorption line is shown in Figure 2, in which panel (a) shows the result of synthesizing the complex of lines at $z = 2.7853$ toward Q0302–003 (with H I column densities decreased by a factor of 100 with respect to the original ones), panel (b) shows the actual components of the Ly α absorption line, and panel (c) shows the result of the Voigt profile fitting procedure. This complex of nine lines is adequately fitted ($\chi^2/\nu = 0.91$) with only three velocity components. The derived spectrum is then fitted in the same way used in § 3.2. The resulting TPCF, Figure 3a, is still weaker than that of the C IV lines, but clearly detectable.

The assumption that all the velocity dispersion is thermal leads to temperatures in excess of $6 \times 10^4 \text{ K}$ in some cases, and this is inappropriate in most models (see Charlton 1995

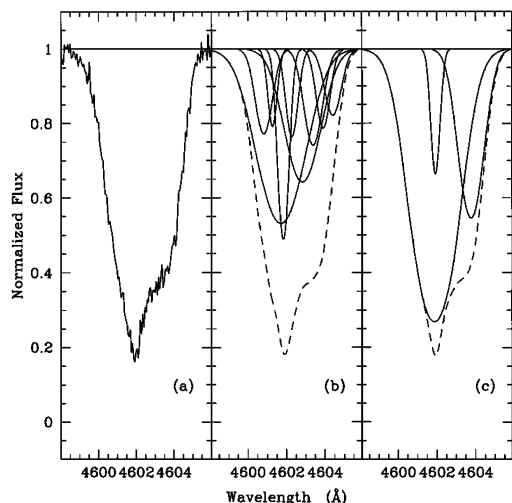


FIG. 2.—Example of how a Voigt profile fit to high spectral resolution, high signal-to-noise ratio observations can underestimate the actual number of velocity components comprising an absorption line. Panel (a) shows the result of synthesizing the complex of lines at $z = 2.7853$ toward Q0302–003 (with H I column densities decreased by a factor of 100 with respect to the original column densities), panel (b) shows the actual components that comprise the Ly α absorption line, and panel (c) shows the result of the Voigt profile fitting procedure.

for a review of the models). We therefore add a second simulation in which the temperature is assumed to be 2×10^4 K, and any excess Doppler parameter is ascribed to turbulence and applied equally to the C IV and Ly α lines. In a few cases the C IV Doppler parameter is just below the assumed thermal value, and in these cases we simply adopt the 2×10^4 thermal width for Ly α . In this simulations the H I column density is assumed to be 10 times that for C IV for each component. The Ly α lines are now generally narrower than in the first simulation, and so the component structure is more easily detected. Consequently, the Ly α line TPCF will have larger values at low velocity separations, as can be seen from Figure 3b. This should be compared with the observational result that little

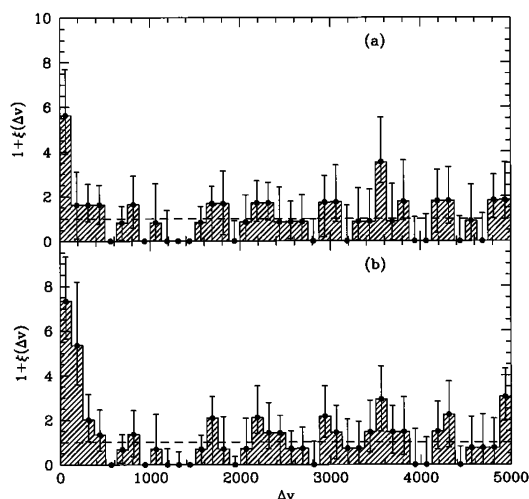


FIG. 3.—The TPCF for low column density clouds [$N(\text{H I}) = \frac{1}{100}$ of CSKH lines] as obtained with two different models: (a) thermal-only broadening (a) and (b) thermal plus turbulence.

clustering is found at these redshifts (see, e.g., Rauch et al. 1992).

These simulations are indeed too naïve, as we are not taking into account the increment in line number density at low column densities. This increment will produce strong blending effects among low column density lines themselves and also with the higher column density lines. Their combined effect is very difficult to simulate, as it depends very strongly on the higher order correlation functions of the distribution of the lines. In addition, there are observations that suggest that the amplitude of the clustering is smaller at these low column densities (Hu et al. 1995). All of these effects could very well erase all the signal in the correlation function for low column density lines, and hence we cannot conclude anything on the behavior of these low column density lines other than it is compatible with being clustered but maybe with a smaller clustering amplitude.

4. DISCUSSION AND SUMMARY

The most significant result of the previous sections is that high-redshift Ly α absorbers with $N(\text{H I}) > 3 \times 10^{14} \text{ cm}^{-2}$ are strongly clustered in redshift on velocity scales $\approx 250 \text{ km s}^{-1}$. While the effect might be due to pairs of clouds with small velocity differences causing the observed TPCF (Miralda-Escudé et al. 1996; Rauch 1996), we could be seeing real clustering. With the observed velocity correlation length we cannot decide whether the Ly α absorbers are independent entities, as has generally been assumed so far, or clouds within the halos of galaxies, the possibility we are exploring here. More detailed questions are even harder to answer—for example, the type of galaxies in which the absorbers might reside, whether we are observing multiple clouds within the same galaxies, and the ionization state of carbon in the clouds. We can only ask if the strength of Ly α clustering is consistent with expectations of galaxy clustering at these early epochs.

To examine this issue, we consider a simple model for the evolution of the galaxy TPCF. In a first step, we ignore peculiar motions and motions of clouds within galaxies and assume that as a function of velocity and redshift the galaxy TPCF can be described by (Efstathiou et al. 1991)

$$\xi(v, z) = (1 + z)^{-3 - \epsilon} \left[\frac{v}{r_0 H(z)} \right]^{-1.8}, \quad (1)$$

where $H(z)$ is the Hubble constant at epoch z (we take $q_0 = 0.5$) and $H_0 r_0 = 550 \text{ km s}^{-1}$ is the present-day galaxy correlation length. The evolutionary parameter ϵ takes the value -1.2 for comoving structures, 0 for virialized clusters, and 0.8 for linearly growing perturbations. Recent theoretical studies (Hamilton et al. 1991; Jain, Mo, & White 1995) show a steeper dependence on redshift at intermediate stages between the linear and virialized limits.

To avoid the divergence of this function at small values of v , we take $\xi(v, z)$ to be constant below a given velocity difference v_0 and equal to $\xi(v_0, z)$. We also convolve it with a Gaussian distribution with width σ to account for random motions. In this way we get a set of different models defined by three parameters, ϵ , σ , and v_0 , which we allow to vary within the limits: $-2 < \epsilon < 4$, $0 < \sigma < 500 \text{ km s}^{-1}$, and $1 < v_0 < 80 \text{ km s}^{-1}$.

Predictions of all these models are then compared with the observed TPCF of high-redshift Ly α absorbers. The best fit is achieved for $\epsilon = 2.4$ and $\sigma = 100 \text{ km s}^{-1}$. The 1, 2, and 3 σ

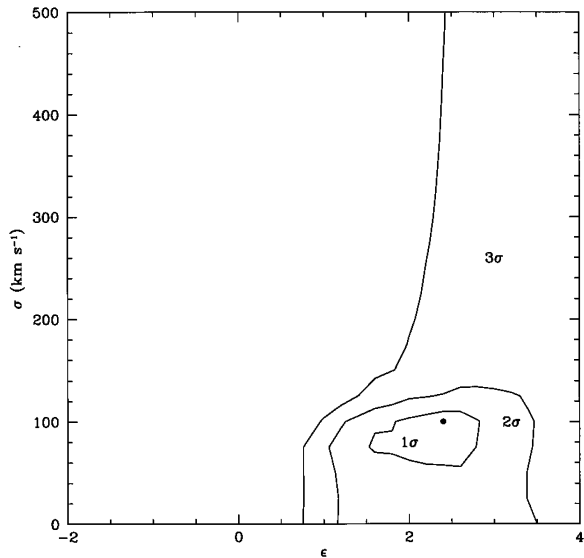


FIG. 4.—Confidence limits in the parameter space formed by the clustering evolution parameter ϵ and the typical velocity of galactic halo motions σ ; 1, 2, and 3 σ confidence contours are plotted.

confidence regions obtained using v_0 as an uninteresting parameter are plotted in Figure 4. From this calculation it is clear that if normal galaxies host the Ly α absorbers, at an average rate of one per galaxy, their correlation function is evolving rapidly and the combined intragalactic and intergalactic velocity dispersion is $\approx 150 \text{ km s}^{-1}$.

Note that our redshift range is relatively small, $\Delta z \approx 0.6$, so that we cannot separately fit r_0 and ϵ . Our determination of ϵ is therefore anchored by the general galaxy correlation function at the present epoch. This may be inappropriate in several

respects. We overestimate the correlation function if the host galaxies of the Ly α clouds are less clustered at the present epoch—for example, if they are mostly spiral galaxies, or we underestimate it if there are multiple Ly α absorbers in galaxies at high redshift. The best we can deduce from our simple analysis is that the observed clustering of high-redshift Ly α absorbers is broadly consistent with the expected clustering of galaxies.

We conclude that (1) high-redshift Ly α absorbers with $N(\text{H I}) > 3 \times 10^{14} \text{ cm}^{-2}$ are strongly clustered in redshift on velocity scales $\lesssim 250 \text{ km s}^{-1}$, (2) previous measurements of the Ly α TPCF have underestimated the actual clustering of the absorbers due to unresolved blending of overlapping velocity components, (3) the present observations may be consistent with the hypothesis that clustering of Ly α absorption systems persists to lower column densities and that likely the clustering is smaller at low column densities, and (4) the observed TPCF is broadly compatible with that expected from galaxies at $z \sim 2-3$.

We interpret these results to suggest that many or most Ly α absorbers may arise in galaxies at all epochs and therefore that the Ly α forest probes the processes of galaxy formation and evolution for redshifts $z \lesssim 5$.

A. F. S. thanks E. Martínez-González for useful discussions and an anonymous referee for calling our attention on the gravitational collapse model. A. F. S. acknowledges support provided by a Spanish MEC studentship. Partial financial support to A. F. S. and X. B. is provided by the Spanish DGICYT under project PB92-0741, K. M. L. is supported by NASA grant NAGW-4433 and by a Career Development Award from the Dudley Observatory, and A. Y. by NASA grant NAG-51228.

REFERENCES

- Bahcall, J., et al. 1996, *ApJ*, 457, 19
 Barcons, X., & Webb, J. K. 1991, *MNRAS*, 253, 207
 Charlton, J. C. 1995, in *QSO Absorption Lines*, ed. G. Meylan (Berlin: Springer), 405
 Cowie, L. L., Songaila, A., Kim, T.-S., & Hu, E. M. 1995, *AJ*, 109, 1522 (CSKH)
 Efstathiou, G., Bernstein, G., Katz, N., Tyson, J. A., & Guhathakurta, P. 1991, *ApJ*, 380, L47
 Hamilton, A. J. S., Kumar, P., Lu, E., & Matthews, A. 1991, *ApJ*, 374, L1
 Hu, E. M., Kim, T. S., Cowie, L. L., Songaila, A., & Rauch, M. 1995, *AJ*, 110, 1526
 Jain, B., Mo, H. J., & White, S. D. M. 1995, *MNRAS* 276, L25
 Lanzetta, K. M., & Bowen, D. V. 1992, *ApJ*, 391, 48
 Lanzetta, K. M., Bowen, D. V., Tytler, D., & Webb, J. K. 1995, *ApJ*, 442, 538
 Miralda-Escudé, J., Cen, R., Ostriker, J. P., & Rauch, M. 1996, *ApJ*, submitted
 Rauch, M. 1996, *Proc. Cold Gas at High Redshift*, ed. M. Bremer et al. (Dordrecht: Kluwer), in press
 Rauch, M., Carswell, R. F., Chaffee, F. H., Foltz, C. B., Webb, J. K., Weymann, R. J., Bechtold, J., & Green, R. F. 1992, *ApJ*, 390, 387
 Sargent, W. L. W., Young, P. J., Boksenberg, A., & Tytler, D. 1980, *ApJS*, 42, 41
 Webb, J. K. 1987, in *Observational Cosmology*, ed. A. Hewitt, G. Burbidge, & L. Z. Fang (Dordrecht: Reidel/Kluwer), 803